

August 1998 • NREL/CP-520-25122

The Morphology, Microstructure, and Luminescent Properties of CdS/CdTe Films

M.M. Al-Jassim, R.G. Dhere, K.M. Jones, F.S. Hasoon, and P. Sheldon



Presented at the 2nd World Conference and Exhibition on
Photovoltaic Solar Energy Conversion; 6-10 July 1998; Vienna, Austria

National Renewable Energy Laboratory
1617 Cole Boulevard
Golden, Colorado 80401-3393
A national laboratory of the
U.S. Department of Energy
Managed by the Midwest Research Institute
For the U.S. Department of Energy
Under Contract No. DE-AC36-83CH10093

THE MORPHOLOGY, MICROSTRUCTURE, AND LUMINESCENT PROPERTIES OF CdS/CdTe FILMS

M.M. Al-Jassim, R.G. Dhere, K.M. Jones, F.S. Hasoon, and P. Sheldon
National Renewable Energy Laboratory, 1617 Cole Blvd., Golden, CO 80401, USA
Phone: (303) 384-6602, Fax: (303) 384-6446, E-mail: mo@nrel.gov

ABSTRACT: This paper is concerned with the characterization of CdS/CdTe polycrystalline thin films for solar cells. The morphology, microstructure, and luminescent properties are studied by a powerful array of characterization techniques. The presence of pinholes in 100-nm thick CdS is observed. The microstructure of CdS and CdTe films is shown to be heavily faulted polycrystalline. The effect of deposition temperature on the grain size and the microstructure is investigated. The interdiffusion of sulfur and tellurium at the CdS/CdTe interface is studied for the first time by a nanoprobe technique. Considerable amount of sulfur is detected in CdTe in the vicinity of the interface of samples deposited at 625°C. The recombination behavior of grain boundaries and intragrain defects is investigated in as-deposited and heat-treated samples.

Keywords: CdTe - 1: Defects - 2: Interface - 3

1. INTRODUCTION

Considerable amount of work has been done on the development of CdS/CdTe solar cells over the last 10 years. However, little has been reported on the microstructure of these films or the recombination behavior of structural defects in them. Further, the interdiffusion issue at the CdS/CdTe interface has so far been studied only by low spatial resolution techniques such as secondary ion mass spectrometry (SIMS) and Auger depth profiling. Preliminary transmission electron microscopy (TEM) investigation [1] showed that CdTe films are heavily faulted with a high density of structural defects. Atomic force microscopy (AFM) examinations proved to be a very powerful approach to study the morphology of as-deposited and heat-treated CdTe films [2]. The CdS/CdTe interface has been a subject of many studies. SIMS was used to study the interdiffusion of sulfur and tellurium [3, 4]. However, SIMS probes relatively large areas and the depth resolution is very sensitive to the surface roughness of the CdTe film. Similarly, X-ray diffraction was extensively used to study the CdS/CdTe interface [5, 6]. Again, this probes relatively large areas and the results can be ambiguous.

In this work, the morphology, microstructure, interface chemistry, and the luminescent properties of the CdS/CdTe system were investigated. The aim in CdS is to optimize the film thickness, grain size, and defect density. In CdTe, the objective is to achieve a better understanding of the nature, generation, three-dimensional distribution, and recombination behavior of structural defects. Further, a direct and unambiguous measurement of interdiffusion at the interface was sought.

2. EXPERIMENTAL

The substrates used in this study were either SnO₂-coated Corning 7059 borosilicate glass, or (100) Si wafers. The latter were used to facilitate TEM cross-sectional sample preparation. The CdS films were grown on these substrates by chemical bath deposition (CBD) using a solution of ammonium acetate, cadmium acetate, thiourea, and ammonium hydroxide in deionized water [7]. The film thickness was varied from 15 to 100 nm by varying the deposition time from 10 to 40 min. Prior to CdTe deposition, the CdS films were heat-treated in a hydrogen ambient for 15 min at 400°C. The CdTe films were deposited by close space sublimation (CSS) in a He/O₂ mixture with a total reactor pressure of 15-30 torr [3]. The substrate temperature varied from 425°-625°C. The source temperature was adjusted to obtain a deposition rate of about 1.5-2 μm/min. CdTe films with a nominal thickness of 3-4 μm were used. The heat treatment was carried out by dipping the CdTe films in CdCl₂/methanol solution (25% to 75% of saturated solutions) for 15 minutes at 55°C, followed by heat treatment at 400°C in a 4:1 volume ratio He/O₂ ambient for 30 min. The film morphology was studied by high resolution, field-emission scanning electron microscopy (FESEM). The structural characterization was carried out by conventional and high resolution TEM. The chemical analysis of the CdS/CdTe interface region was performed in a field-emission analytical TEM using energy-dispersive X-ray spectroscopy (EDS) analysis. The probe size used was in the 1-2 nm range. The recombination behavior of structural defects, such as grain boundaries, was probed using room-temperature cathodoluminescence imaging in a conventional SEM.

3. CdS

The CdS grain size was studied as a function of film thickness. Fig. 1 shows a CdS film deposited for 15 min, resulting in a film thickness of approximately 40 nm. The average grain size in this film is approximately 30 nm which corresponds to the film thickness. However, increasing the film thickness to 100 nm did not give rise to a linear increase in grain size. This is illustrated in Fig. 2, which is a FESEM micrograph of a 100 nm thick film, exhibiting an average grain size of 60 nm.

One of the main objectives of this study is to establish the minimum CdS film thickness at which a continuous film is achieved. Examining the thinnest sample (10-min deposition, 20-nm film) indicated that large areas of the SnO₂ film are covered by CdS. However, the coverage is not complete. Increasing the deposition time to 15 min resulted in a higher surface coverage. Nonetheless, two undesirable features were clearly revealed by FESEM. The first is gross discontinuities in the CdS film, and the second is a high density of pinholes (Fig. 1). The size of the gross discontinuities observed was up to 10 μm. What we refer to as pinholes here, however, are features on the order of a micron or less. As the deposition time increased, both the size of the discontinuities and their density decreased. At 30 min of deposition, the large discontinuities shrunk in size to the 1-2 μm range, and the density of the pinholes decreased significantly. At 35 min of deposition, the film thickness is ~100 nm. The gross film discontinuities are virtually absent, but pinholes are still clearly evident. Increasing the deposition time to 40 min or more resulted in undesirable film properties, such as the deposition of fine-grain material on the film's surface and the incorporation of particles in the film. These particles are believed to be caused by homogeneous nucleation of CdS in the solution.

The chemical properties of the gross discontinuities were investigated by Auger electron spectroscopy (AES). Such analysis revealed that many of these discontinuities are bare SnO₂ film. This is indicative of a lack of CdS nucleation in these areas. Such a nucleation could have been inhibited by the contamination of these areas on the SnO₂ film surface. Other AES analyses showed that some of these areas comprise a thinner CdS film than the matrix. This was clearly shown in AES surveys taken within and adjacent to one of these regions. Both analyses revealed CdS; However, after a short 1-min sputter, only SnO₂ signal was detected from the defective region. This is clearly indicative of the low CdS film thickness in these regions. Furthermore, AES analyses revealed the presence of oxygen and carbon in many of these regions. This supports the hypothesis that this type of defects is caused by contamination. The latter is likely to

originate from impurity species in the chemical bath itself [8].

4. CdTe

TEM cross-sectional examination was performed on CdTe films deposited at different temperatures

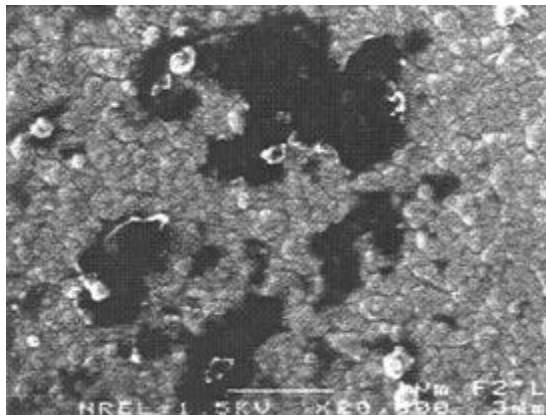


Figure 1: SEM micrograph of a 40-nm thick CdS Film, showing gross discontinuities and pinholes.

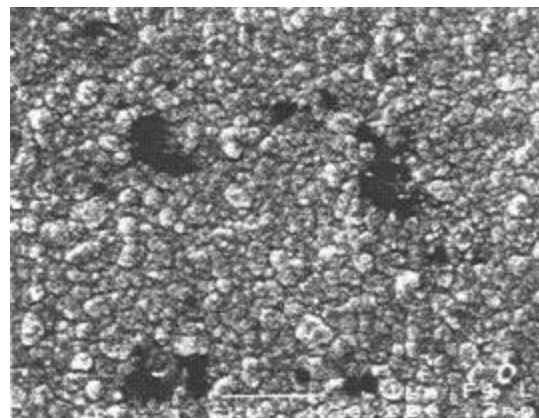


Figure 2: SEM micrograph of a 100-nm thick CdS Film, showing pinholes.

[Fig. 3]. The grain size in as-deposited CdTe increased significantly with increasing substrate temperature. However, no correlation was observed between the grain size of the CdTe and that of the underlying CdS. This is contrary to our previous findings on CdTe deposited by physical vapor deposition [1]. We believe this results from the CSS deposition being a higher temperature process, with a higher surface mobility during growth.

As-deposited CdTe films were found to be heavily faulted with a high density of planar defects and threading dislocations. Fig. 3 shows TEM

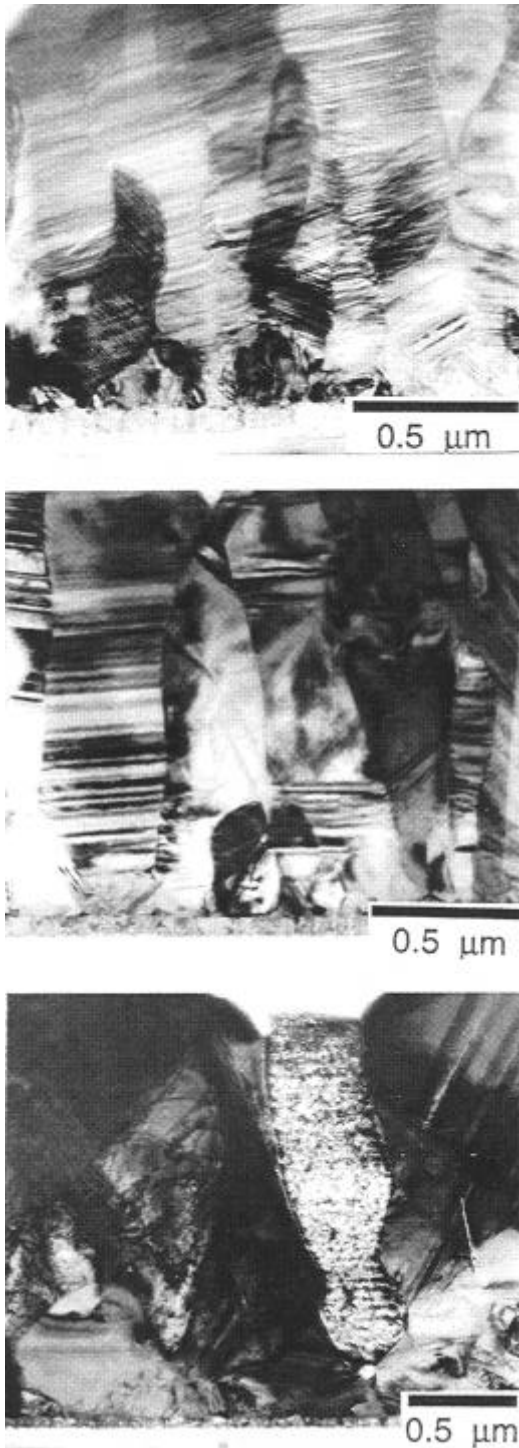


Figure 3: TEM cross-sections of CdTe films deposited at: top, 425°C; middle, 525°C; and bottom, 625°C.

cross-sections of CdTe films deposited at 425, 525 and 625°C. This figure clearly shows the high density and the three-dimensional distribution of planar defects. These defects are primarily stacking faults and micro-twins on {111} planes. Their density, however, varies from one grain to another. Additionally, cross-sectional examination revealed

that the defect density decreases as the film thickness increases. We believe this is largely due to the annihilation of stacking faults as a result of interaction on intersecting {111} planes.

However, the defect density is not affected by substrate temperature. Furthermore, high-resolution investigation of the CdS/CdTe interface region in CdCl₂-treated samples revealed a very complex defect structure. An extremely high density of stacking faults was observed in the vicinity of the interface. This is believed to be caused by the sulfur diffusion into CdTe and the alloying of the interface region. We observed that the composition of this CdS_xTe_{1-x} interface alloy is very non-uniform. Therefore, it is conceivable that the boundary between the cubic tellurium rich CdS_xTe_{1-x} and the hexagonal sulfur rich CdS_xTe_{1-x} is a stacking fault.

EDS elemental analysis was performed on samples deposited at 425° and 625°C with no heat treatment. The analyses were carried out using line scans and stationary probe. In the linescan analysis mode, a 2-nm probe was moved across the interface region in 2-nm increments. The dwell time on each point was set at 100 s to achieve good counting statistics. Cd, Te, and S were analyzed and plotted as a function of position. Fig. 4 shows such analysis for the sample deposited at 425°C. Clearly, the interface is fairly abrupt with an interface width on the order of 25 nm. EDS analysis of the sample with a CdTe film deposited at 625°C revealed startlingly different results (Table I). Stationary probe analysis was performed at 20nm from the interface, and 1.5 μm away. Clearly, a considerable amount of sulfur is diffusing into CdTe giving rise to what is believed to be an alloyed CdS_xTe_{1-x} region. The extent of this region and how that is affected by deposition and post-deposition treatment is currently being investigated.

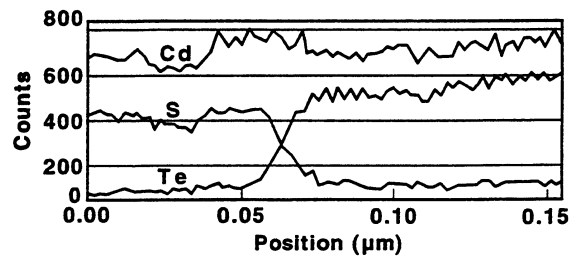


Figure 4: High resolution EDS elemental line-scans across the interface of a 425°C sample.

Table I: EDS chemical analysis of CdTe.

	Near Interface	1.5 μm away
Cd	51.45%	52.29%
Te	38.31%	46.65%
S	10.24%	1.05%

Cathodoluminescence (CL) imaging was performed on as-deposited and CdCl₂-treated samples in both plan-view and cross-sectional configuration. To minimize the error in estimating the carrier recombination efficiency at defect sites, linescan measurements were performed. However, it must be cautioned here that the effect of surface topography could not be eliminated. Fig. 5 shows a CL linescan across an as-deposited CdTe film revealing a very high degree of non-radiative recombination at grain boundaries and at intragrain defects. Fig. 6 is a similar CL linescan on the same sample after CdCl₂ treatment. This indicates a factor of two reduction in the recombination efficiency at grain boundaries and at intragrain defects. This is clearly indicative of the passivating effect of the CdCl₂ treatment.

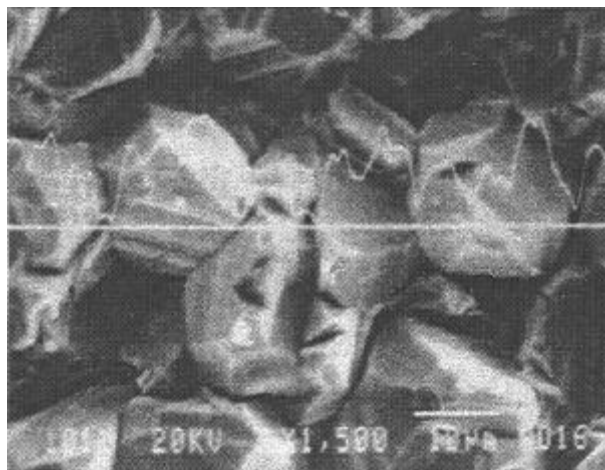


Figure 5: CL linescan superimposed on an SEM image of an as-deposited CdTe film.

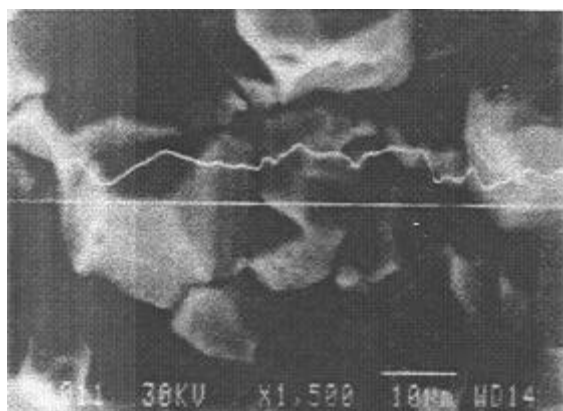


Figure 6: CL linescan superimposed on an SEM image of the CdTe film shown in Fig. 5 after CdCl₂ treatment

5. SUMMARY

All CdS films examined in this study exhibited pinholes and discontinuities varying in size and density. This could have a significant impact on

cell performance, as these pinholes could provide shunting paths between the CdTe and the SnO₂. The CdS grains are heavily faulted, with a high density of stacking faults. This will have a deleterious effect on the CdS/CdTe interface region, as we have shown in a previous study that planar defects in CdS tend to propagate into the CdTe films. Most CdTe grains are heavily faulted, with a high density of dislocations, stacking faults and twins. The defect density varied from one grain to another. However, the density is not significantly affected by substrate temperature. Hence, the widely observed improvement in device performance with increasing substrate temperature is not caused by a reduction in structural defect density.

This study clearly revealed that grain boundaries and intragrain defects in CdTe act as active non-radiative recombination sites. CL examination showed that CdCl₂ treatment markedly lowers the recombination efficiency of grain boundaries, and intragrain defects in CdTe.

At deposition temperatures below 450°C, only small amounts (~1%) of sulfur were detected in the CdTe films in the vicinity of the interface. In CdTe films deposited at 625°C, on the other hand, sulfur levels exceeding 10% were detected. This clearly indicates that CdTe devices deposited at high temperatures have an alloyed (CdS_xTe_{1-x}) active region.

ACKNOWLEDGMENT

This work was performed for the U.S. Department of Energy under contract No. DE-AC36-83CH10093.

REFERENCES

- [1] M.M. Al-Jassim, F.S. Hasoon, K.M. Jones, B.M. Keyes, R.J. Matson, H.R. Moutinho, Proceedings 23rd IEEE PVSC conf. (1993) 459.
- [2] H.R. Moutinho, M.M. Al-Jassim, D.H. Levi, P.C. Dippo, L.L. Kazmerski, J. Vac. Sci. Technol. A **16** (1998) 1251.
- [3] R.G. Dhere, D.S. Albin, D.H. Rose, S.E. Asher, K.M. Jones, M.M. Al-Jassim, Material Res. Soc. Proc. **426** (1996) 361.
- [4] S.E. Asher, Proceedings Microbeam Analysis (1990) 97.
- [5] B.E. McCandless, R.W. Birkmire, Proceedings of the 14th Photovoltaic Program Review, Denver, CO, 1996, AIP Conference Proceedings **394** (1996) 647.
- [6] I. Clemminck, M. Burgelman, M. Casteleyn, J. De Poorter, A. Vervae, Proceedings 22nd IEEE PVSC conf. (1991) 1114.
- [7] F.S. Hasoon, M.M. Al-Jassim, A. Swartzlander, P. Sheldon, Proceedings 26th IEEE PVSC conf. (1997) 459.
- [8] J.D. Webb, D.H. Rose, D.W. Niles, A. Swartzlander, M.M. Al-Jassim, Proceedings 26th IEEE PVSC conf. (1997) 399.